

AD \_\_\_\_\_

Award Number: W81XWH-06-1-0749

TITLE: Harnessing Functional Genomics to Reverse Chemoresistance in Breast Cancer

PRINCIPAL INVESTIGATOR: Brian Bodemann

CONTRACTING ORGANIZATION: University of Texas Southwestern Medical Center  
Dallas, TX 75390

REPORT DATE: October 2007

TYPE OF REPORT: Annual Summary

PREPARED FOR: U.S. Army Medical Research and Materiel Command  
Fort Detrick, Maryland 21702-5012

DISTRIBUTION STATEMENT: Approved for Public Release;  
Distribution Unlimited

The views, opinions and/or findings contained in this report are those of the author(s) and should not be construed as an official Department of the Army position, policy or decision unless so designated by other documentation.

REPORT DOCUMENTATION PAGE				Form Approved OMB No. 0704-0188	
Public reporting burden for this collection of information is estimated to average 1 hour per response, including the time for reviewing instructions, searching existing data sources, gathering and maintaining the data needed, and completing and reviewing this collection of information. Send comments regarding this burden estimate or any other aspect of this collection of information, including suggestions for reducing this burden to Department of Defense, Washington Headquarters Services, Directorate for Information Operations and Reports (0704-0188), 1215 Jefferson Davis Highway, Suite 1204, Arlington, VA 22202-4302. Respondents should be aware that notwithstanding any other provision of law, no person shall be subject to any penalty for failing to comply with a collection of information if it does not display a currently valid OMB control number. <b>PLEASE DO NOT RETURN YOUR FORM TO THE ABOVE ADDRESS.</b>					
1. REPORT DATE 01-10-2007		2. REPORT TYPE Annual Summary		3. DATES COVERED 15 Sep 2006 – 14 Sep 2007	
4. TITLE AND SUBTITLE  Harnessing Functional Genomics to Reverse Chemoresistance in Breast Cancer				5a. CONTRACT NUMBER	
				5b. GRANT NUMBER W81XWH-06-1-0749	
				5c. PROGRAM ELEMENT NUMBER	
6. AUTHOR(S)  Brian Bodemann  Email: <a href="mailto:brian.bodemann@utsouthwestern.edu">brian.bodemann@utsouthwestern.edu</a>				5d. PROJECT NUMBER	
				5e. TASK NUMBER	
				5f. WORK UNIT NUMBER	
7. PERFORMING ORGANIZATION NAME(S) AND ADDRESS(ES)  University of Texas Southwestern Medical Center Dallas, TX 75390				8. PERFORMING ORGANIZATION REPORT NUMBER	
9. SPONSORING / MONITORING AGENCY NAME(S) AND ADDRESS(ES) U.S. Army Medical Research and Materiel Command Fort Detrick, Maryland 21702-5012				10. SPONSOR/MONITOR'S ACRONYM(S)	
				11. SPONSOR/MONITOR'S REPORT NUMBER(S)	
12. DISTRIBUTION / AVAILABILITY STATEMENT Approved for Public Release; Distribution Unlimited					
13. SUPPLEMENTARY NOTES					
14. ABSTRACT  Targeted therapy has proven to be an effective strategy in the treatment of breast cancer. An example of successful targeted therapy is trastuzumab, a humanized monoclonal antibody binds to the extracellular domain of HER2, a receptor which is overexpressed in many breast cancers. The goal of my project is to identify molecular targets for conjunctive therapy that will increase efficacy of trastuzumab therapy. To identify molecular targets necessary for breast cancer cell survival in the presence of trastuzumab, a breast cancer cell line with known cytostatic sensitivity to trastuzumab, will be screened using a high throughput assay using a with a unique small interfering (si)RNA library targeting all 21,125 known genes in the human genome database. This information will help identify new synergistic combinations with existing drugs and novel therapeutic targets that can act synergistically as initial therapy and upon the development of resistance. During the time covered by this annual summary, I have made major progress towards fulfilling my training requirements and finished optimizing conditions for the execution of this screen as outlined in AIM1.					
15. SUBJECT TERMS Genomics, breast, cancer, siRNA, screen, Herceptin, trastuzumab					
16. SECURITY CLASSIFICATION OF:			17. LIMITATION OF ABSTRACT	18. NUMBER OF PAGES	19a. NAME OF RESPONSIBLE PERSON
a. REPORT	b. ABSTRACT	c. THIS PAGE			USAMRMC
U	U	U	UU	20	19b. TELEPHONE NUMBER (include area code)

## Table of Contents

	<u>Page</u>
<b>Introduction</b>	<b>4</b>
<b>Body</b>	<b>5</b>
<b>Key Training Accomplishments</b>	<b>12</b>
<b>Key Research Accomplishments</b>	<b>12</b>
<b>Reportable Outcomes</b>	<b>N/A</b>
<b>Conclusion</b>	<b>12</b>
<b>References</b>	<b>13</b>
<b>Appendices</b>	<b>14</b>

## INTRODUCTION

Targeted therapy has proven to be an effective strategy in the treatment of breast cancer. An example of successful targeted therapy is trastuzumab (Herceptin), a recombinant DNA-derived humanized monoclonal antibody that selectively binds with high affinity to the extracellular domain of HER2, a receptor which is overexpressed in many breast cancers [1,2]. In clinical trials patients who received trastuzumab in combination with standard combination chemotherapy had a significant decrease in disease recurrence compared to patients treated with chemotherapy alone [3,4,5]. Unfortunately, the majority of patients who achieve an initial response to trastuzumab-based regimens generally acquire resistance within 1 year [6,7]. The goal of my project is to identify molecular targets for conjunctive therapy that will increase the cell autonomous efficacy of trastuzumab therapy and potentially switch trastuzumab to a cytotoxic drug *in vitro*. To identify molecular targets necessary for breast cancer cell survival in the presence of trastuzumab, the human breast cancer cell line, BT474, with known cytotoxic sensitivity to trastuzumab, will be screened using a high throughput assay using a unique small interfering (si)RNA library targeting all 21,125 known genes in the human genome database. A screen that looks for much greater reduction in cell number than seen with trastuzumab therapy alone will be conducted in the presence of drug in microtiter plates with a robotic high throughput screening system. We have recently validated this high throughput approach in a screen of non-small cell lung cancer to identify molecular targets which sensitize cells to the anti-cancer drug paclitaxel [8]. Phenomena that occur in traditional adherent culture do not always reproduce *in vivo*; therefore, a few promising hits will be further analyzed in an organotypic 3-dimensional cell culture system that better models the tumor microenvironment. Our approach will facilitate the unbiased and unambiguous identification of key proteins and pathways selectively required for survival of breast cancer cells upon exposure to trastuzumab. This information will help identify new synergistic combinations with existing drugs and novel pharmaceutically tractable therapeutic targets that can act synergistically as initial therapy and upon the development of resistance.

## BODY

During the first year of this fellowship I have focused on the following: 1) Completion of my graduate school core coursework and training requirements together with completion of my graduate program course requirements and preliminary exam. I have now advanced to full candidacy for the Ph.D. in Cell Regulation program. 2) Publication of a manuscript describing the first human genome-wide siRNA screen. 3) Development of an effective high throughput assay platform for BT474 sensitivity to Herceptin. 4) Development of an experimental system to control for altered drug sensitivity within “organotypic” culture environments.

1. My graduate training accomplishments are bulleted below.
2. My first publication, supported in part by this fellowship, is included in the appendix.
3. Work to have been completed:

AIM1A and AIM1C:

In order to effectively screen BT474 cells for the consequence of individual depletion of over 21,000 genes on cell proliferation and survival in the presence and absence of Herceptin, a highly reproducible and effective protocol must be established using automated liquid handlers and simple quantitative end-point assays. We are employing a Biomek FX for delivery of siRNAs into assay plates and Titertek multidrops for delivery of transfection reagents, cells and media, as well as for delivery of the drug and end-point assay cocktail. First, I identified the constraints with respect to volumes and surface areas that will allow reproducible and accurate delivery of reagents with this equipment. Next, I developed transfection protocols and an assay platform that works within these restraints as described below. The protocols used for optimization are attached in the appendices.

I have attached Figures 1 through 4, which summarize the positive and negative results of these experiments

Figure 1: Dharmafect-2 is an effective transfection agent at 0.05 $\mu$ L and 0.1 $\mu$ L per well

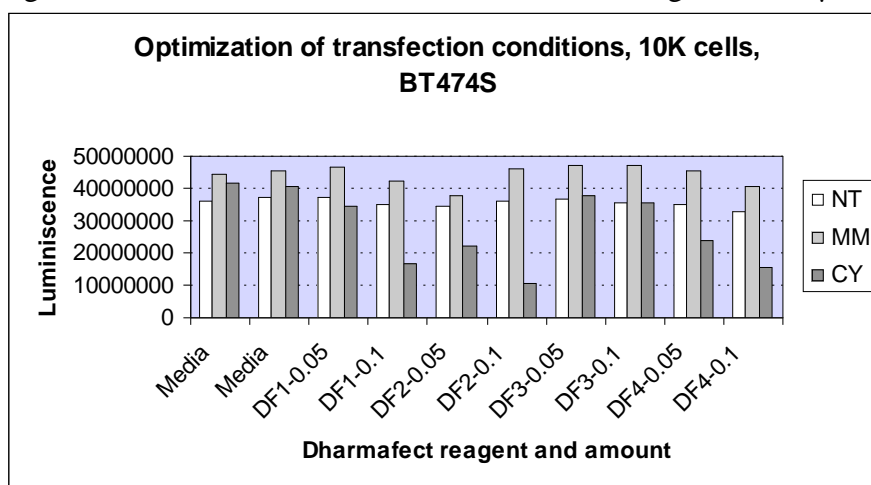


Figure 2: Dharmafect 1,2,3 and 4 are all effective reagents at 0.2μL per well, but Dharmafect-2 exhibits non-specific cytotoxicity at 0.3μL per well.

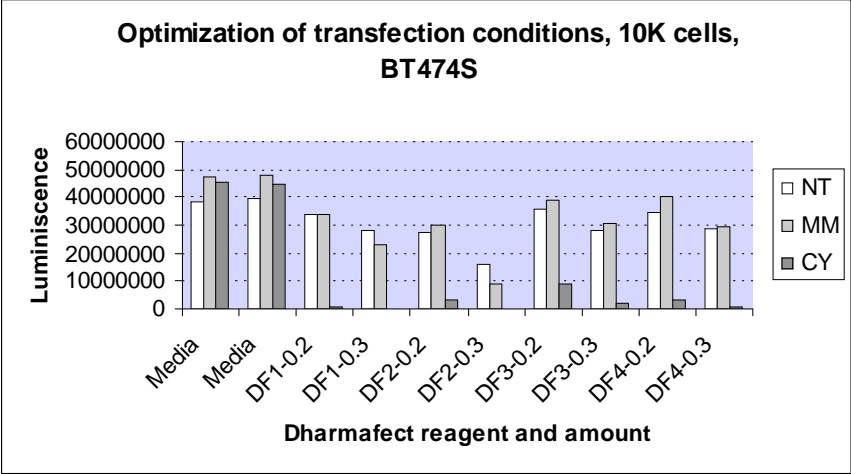


Figure 3: Dharmafect-2 exhibits a dose-dependent transfection of BT474 cells as measured by Cytotoxic oligo induced cell death.

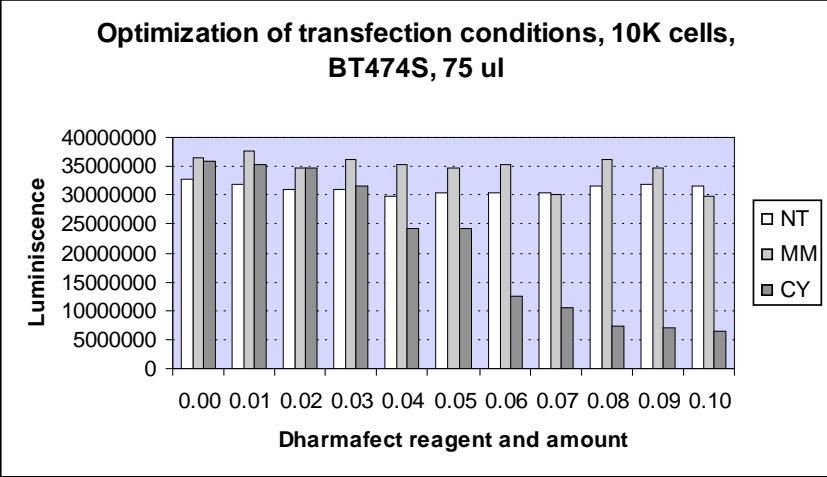
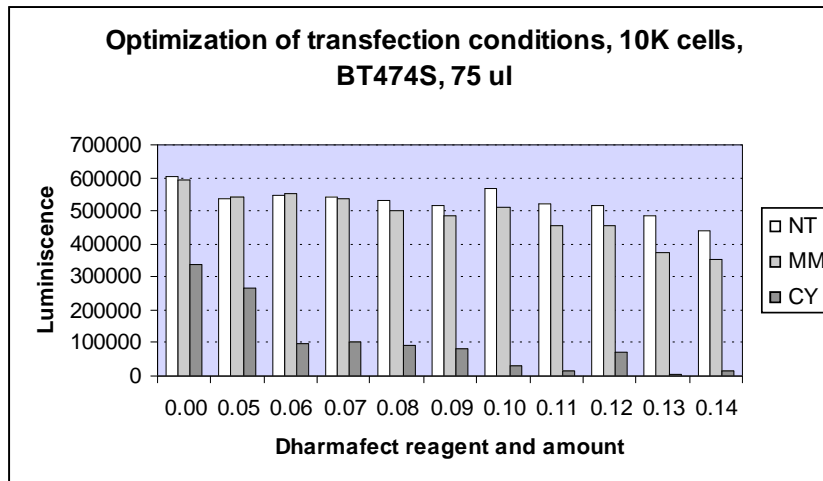


Figure 4: Dharmafect-2 exhibits a dose-dependent transfection of BT474 cells as measured by Cytotoxic oligo induced cell death.



#### Summary of Transfection Optimization:

In Figures 1 and 2, we identified that Dharmafect-2 (DF2) as the optimal reagent for transfecting BT474 cells. In Figures 3 and 4 we have identified that as little as 0.06  $\mu$ L of Dharmafect-2 per well can be utilized to transfect BT474 cells. The experiments presented in Figures 1 through 4 have allowed us to identify a cost effective protocol for delivery of siRNA duplexes into BT474 breast cancer cells. We will utilize this protocol in our optimized HTS platform, which is summarized below.

#### Optimized HTS platform:

For each of the 267 master plates:

1. Load 175 ul media into Assay Plate 1 with Titertek multidrop.
2. Deliver siRNA from stock plate into Assay Plate 1 with Biomek FX.
3. Mix and distribute 30ul of media/siRNA mixture to Assay plates 2-6 with Biomek FX.
4. Add 10ul per well of transfection reagent to each assay plate with Titertek multidrop.
5. Add 10,000 cell/well to each assay plate with Titertek multidrop.
6. 48 hours post transfection, exchange media using a Hydra-96 together with the multidrop in plates 1-3 with fresh media+Herceptin, and in plates 4-6 with fresh media+solvent.
7. 48 hours post drug delivery add CTG with Titertek multidrop.

Figure 5 summarizes this platform in a flowchart.

**267 plates, 80 compounds/plate\***

**Stock**  
2 nmoles

MD: 200 ul

**Stock**  
10 uM in 200 ul

FX - 50 ul/well

**Master 1**  
10 uM in 50 ul  
Diluted to 100 ul (5.0 uM)  
(conical)

**Master 2 (conical)**  
10 uM in 50 ul

**Master 3 (conical)**  
10 uM in 50 ul

**Master 4 -light (conical)**  
10 uM in 50 ul

Banked in Freezers XYZ

FX : ②  
10 ul/well

**Assay (plate 1 of 6)**

MD: 10 ul  
RPMI/Dfect 1

FX : ③  
30 ul/well (Sul 'play')

**Assay (6)**  
8.3 pmoles/40 ul

④

**Assay (6)**  
8.3 pmoles/30 ul  
(5 flat-bottom plates)

⑤

MD: 160 ul cells

**Assay (6)**

⑥

PW: Xchange  
150ul RPMI  
For 50ul +/- Herceptin

**Assay (3) carrier 100ul**

**Assay (3) 10nM Herceptin 100ul**

⑦

MD: 15 ul  
CTG/well

Read Plates

①

MD: 175 ul  
RPMI/well

**Assay (plate 1 of 6)**

1 flat-bottom plate)  
Apply unique barcode



AIM1B. We determined the optimal concentration of Herceptin to achieve a 25% growth delay in BT474 cells. A dose of 0.1 $\mu$ g/mL of Herceptin achieved this result when 1,000 BT474 cells were plated in 96-well plate. A representative experiment is shown in Figure 6. We then tried this assay with 10,000 cells per well as we planned to use during primary screen. Figure 7 illustrates a representative experiment where we see that 10,000 cells is inappropriate for deriving a 25% growth delay with Herceptin treatment. Because transfection will reduce the cell number due to non-specific cytotoxicity, we next tested Herceptin treatment combined with reverse transfection of siRNA with Dharmafect-2. Figure 8 illustrates that 10,000 cells is appropriate when paired with transfection. Also, siRNA-mediated depletion of the chemokine receptor CXCR4 (a candidate sensitizer to Herceptin) resulted in enhanced sensitivity to Herceptin at both 1 and 10 $\mu$ g/mL doses. This experiment validated that we had finally established a 96-well assay, which can effectively interrogate the importance of a candidate Herceptin sensitizer.

Figure 6: 0.25 $\mu$ g/mL Herceptin achieves >25% growth delay in 1,000 BT474 cells

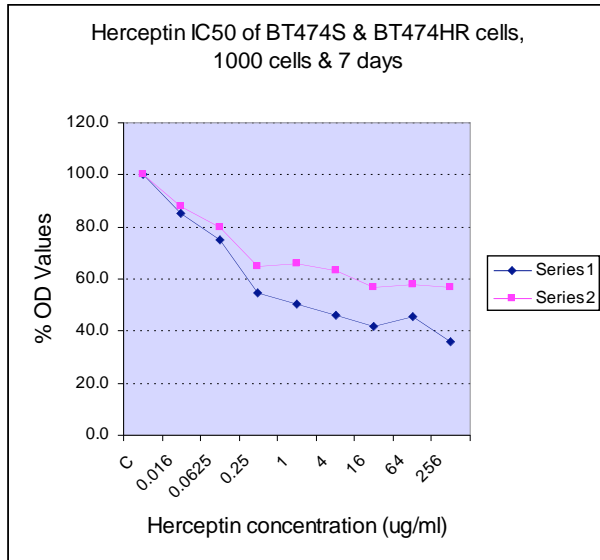


Figure 7: 10,000 BT474 cells per well limits herceptin efficacy in 96-well format.

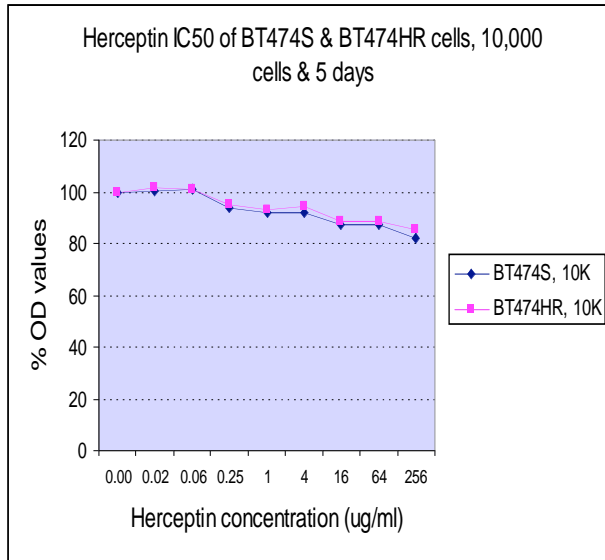
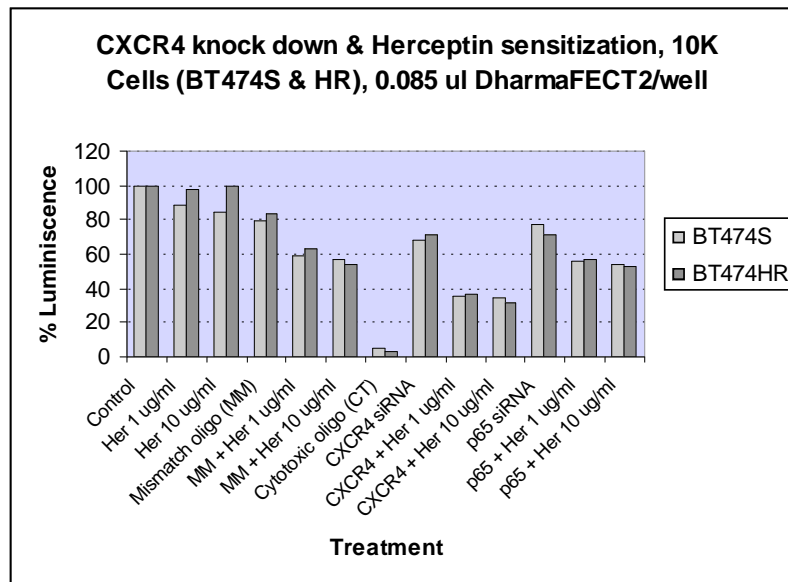


Figure 8: CXCR4 knockdown sensitizes BT474 cells to Herceptin treatment in our 96-well assay.



## AIM1 ISSUES

Execution of AIM1 while also undergoing classwork and the rigorous qualifying exam procedure for the Cell Regulation Ph.D. program proved to be incompatible. Therefore, during the three months of the qualifying exam procedure only minimal progress was made on AIM1. After completion of the first genome wide siRNA screen in human cells [8], we learned some important caveats to consider when identifying an effective high-throughput protocol for reverse transfection of BT474 breast cancer cells: 1. efficacy and 2. cost-effectiveness. The difference between 0.085 $\mu$ L per well and 0.3 $\mu$ L per well when applied over 22,000 assays can represent a substantial cost to the investigator. For this

reason, we took great care investigate very low levels of transfection agent. This substantially increased the time of execution for AIM1, but will represent a substantial gain in reduction of cost of execution in the primary screen.

#### **AIM1 SUMMARY**

We have completed AIM 1A, 1B, and 1C by identifying the optimal transfection, herceptin treatment conditions of BT474 cells for execution of a high-throughput screen.

#### **AIM2 ISSUES**

The primary screen, which was described in AIM2 of the proposal, was also to be begun during year one. Unfortunately, AIM1 was significantly delayed as described above under AIM1 ISSUES. However, the most tedious part of preparing for a primary screen of this magnitude is making certain that your assay is capable of generating a large enough dynamic range, so that novel genetic relationships with Herceptin can generated. Figure 8 illustrates clearly that we have reached this endpoint in assay development and are now ready to move forward with the primary screen described in AIM2.

## **KEY TRAINING ACCOMPLISHMENTS**

1. I finished the class work necessary for my doctorate by completing the Signal Transduction course.
2. I prepared a written qualifying exam proposal, and I passed both the written and oral defense portions of the qualifying exam proposal.
3. I participated in two Journal Clubs in Cell Regulation training program during the Fall and Spring semesters.
4. I presented my research in a Works in Progress seminar series that was attended by faculty and students from Cell Regulation training program.
5. I presented my research in a Works in Progress seminar series that was attended by the directing faculty and students from Medical Scientist Training Program.
6. I presented my research at the annual retreat of the Medical Scientist Training Program (MSTP) at UT Southwestern, which was attended by the directing faculty of the MSTP, students from the MSTP, and invited faculty from UT Southwestern.

## **KEY RESEARCH ACCOMPLISHMENTS**

1. I have participated as a coauthor in the completion and publication of the first human genome-wide siRNA screen[8].
2. A high-throughput compatible experimental platform has been developed to interrogate BT474 responses to Herceptin.
3. The chemokine receptor CXCR4 has been identified as a target for sensitizing breast cancer cells to Herceptin.

## **CONCLUSIONS**

I have advanced on schedule with my graduate program training requirements. We completed AIM1 and have developed an effective high-throughput siRNA screening platform for interrogating novel genetic relationships with Herceptin in BT474 breast cancer cells. We have validated our protocol and identified CXCR4 as a potential drug target for sensitization of breast cancer cells to Herceptin treatment. This is a big step forward as inhibitors of this receptor are already in drug development to slow the spread of HIV infection.

## REFERENCES

- [1] Slamon, D. J., G. M. Clark, et al. (1987). "Human breast cancer: correlation of relapse and survival with amplification of the HER-2/neu oncogene." Science **235**(4785): 177-82.
- [2] Slamon, D. J., W. Godolphin, et al. (1989). "Studies of the HER-2/neu proto-oncogene in human breast and ovarian cancer." Science **244**(4905): 707-12.
- [3] **NSABP-B-31:** Phase III Randomized Study of Doxorubicin and Cyclophosphamide Followed By Paclitaxel With or Without Trastuzumab (Herceptin) in Women with Node-Positive Breast Cancer That Overexpresses HER2.
- [4] **NCCTG-N9831:** Phase III Randomized Study of Doxorubicin Plus Cyclophosphamide Followed By Paclitaxel With or Without Trastuzumab (Herceptin®) in Women with HER-2-Overexpressing Node-Positive or High-Risk Node-Negative Breast Cancer.
- [5] Romond, E. H., E. A. Perez, et al. (2005). "Trastuzumab plus adjuvant chemotherapy for operable HER2-positive breast cancer." N Engl J Med **353**(16): 1673-84.
- [6] Cobleigh, M. A., C. L. Vogel, et al. (1999). "Multinational study of the efficacy and safety of humanized anti-HER2 monoclonal antibody in women who have HER2-overexpressing metastatic breast cancer that has progressed after chemotherapy for metastatic disease." J Clin Oncol **17**(9): 2639-48.
- [7] Vogel, C. L., M. A. Cobleigh, et al. (2002). "Efficacy and safety of trastuzumab as a single agent in first-line treatment of HER2-overexpressing metastatic breast cancer." J Clin Oncol **20**(3): 719-26.
- [8] Whitehurst, A.W., B. O. Bodemann, et. al. (2007) "Synthetic lethal screen identification of chemosensitizer loci in cancer cells." Nature **446**(7137): 815-819.

## APPENDICES

1. The materials/protocols utilized for optimization of AIM1A and AIM1C are attached as page 15.
2. To illustrate our progress in performing projects of this magnitude, our 2007 Nature paper for which I was a co-author, “Synthetic lethal screen identification of chemosensitizer loci in cancer cells.”, is attached as pages 16 to 20.

## AIM1A/C: Transfection Optimization Protocol

### Materials:

- 96 well plates: White-walled, clear bottom sterile with cover from Corning #3903
  - Dharmafect Reagents 1-4 (can be bought as set of 4 from Dharmacon)
  - Control siRNAs
    - siControl non-targeting siRNA #1-4 (bought as pool) D-001206-13-05 (designated “MM” below)
    - PLK1 pool from Dharmacon - MU-003290-01
    - siControl TOX from Dharmacon D-001500-01-05 (designated “CY” below)
- Dilute all siRNA to a final concentration of 10 uM (water may be used). Store at -80 in 25-50 ul aliquots.
- CellTiterGlo Reagent from Promega (can be aliquoted in single use amount (1ml) and frozen) G7572
  - MultiDrop or Multichannel Pipetman
  - Standard EOC media, trypsin, 1X PBS

### Procedure:

#### A). Make 2 Sets of Master Mixes:

- 1). Oligo Master Mix (3 tubes); 464 ul Serum Free Medium (EOC) + 16 oligo: manually pipet 30 ul/well (see chart below)
- 2). Dharmafect Master Mix: two ratios for each reagent: 0.2 and 0.4 (8 tubes total)

0.2 Mix: 1.2 DF X + 58.8 Serum Free Medium (EOC)

0.4 Mix: 2.4 DF + 57.6 Serum Free Medium (EOC)

Manually pipet 10 ul master mix #2 to appropriate well (see chart below).  
Incubate for 20 minutes.

B) Split cells and count them. Dilute cells to ~62,500/ml. Add 160 ul of the dilution to each well using a multidrop or multichannel pipetman. (this step is performed in regular, serum containing medium). This method gives a total of 10,000 cells/well in a volume of 200 ul. Sometimes cells will grow to fast the and the # of cells plates will have to altered to find the optimal transfection amount – but 10,000 is usually a good starting point.

C) Spin cells at 500 x g for 1 min to facilitate even spreading. Incubate for 96 hours at 37 C.

D) To read plates, add 15 ul of Cell Titer Glo reagent, agitate for 2 minutes, incubate for 10 minutes and read with a plate reader equipped with a luminometer. Raw numbers are proportional to the amount of cells in each well.

# Synthetic lethal screen identification of chemosensitizer loci in cancer cells

Angelique W. Whitehurst<sup>1</sup>, Brian O. Bodemann<sup>1</sup>, Jessica Cardenas<sup>1</sup>, Deborah Ferguson<sup>2</sup>, Luc Girard<sup>3</sup>, Michael Peyton<sup>3</sup>, John D. Minna<sup>3,4</sup>, Carolyn Michnoff<sup>5</sup>, Weihua Hao<sup>5</sup>, Michael G. Roth<sup>5</sup>, Xian-Jin Xie<sup>4,6</sup> & Michael A. White<sup>1,4</sup>

Abundant evidence suggests that a unifying principle governing the molecular pathology of cancer is the co-dependent aberrant regulation of core machinery driving proliferation and suppressing apoptosis<sup>1</sup>. Anomalous proteins engaged in support of this tumorigenic regulatory environment most probably represent optimal intervention targets in a heterogeneous population of cancer cells. The advent of RNA-mediated interference (RNAi)-based functional genomics provides the opportunity to derive unbiased comprehensive collections of validated gene targets supporting critical biological systems outside the framework of preconceived notions of mechanistic relationships. We have combined a high-throughput cell-based one-well/one-gene screening platform with a genome-wide synthetic library of chemically synthesized small interfering RNAs for systematic interrogation of the molecular underpinnings of cancer cell chemoresponsiveness. NCI-H1155, a human non-small-cell lung cancer line, was employed in a paclitaxel-dependent synthetic lethal screen designed to identify gene targets that specifically reduce cell viability in the presence of otherwise sublethal concentrations of paclitaxel. Using a stringent objective statistical algorithm to reduce false discovery rates below 5%, we isolated a panel of 87 genes that represent major focal points of the autonomous response of cancer cells to the abrogation of microtubule dynamics. Here we show that several of these targets sensitize lung cancer cells to paclitaxel concentrations 1,000-fold lower than otherwise required for a significant response, and we identify mechanistic relationships between cancer-associated aberrant gene expression programmes and the basic cellular machinery required for robust mitotic progression.

Paclitaxel and related taxanes are routinely used in the treatment of non-small-cell lung cancer (NSCLC) and other epithelial malignancies. Although objective responses and survival benefits are seen, complete responses are uncommon. Half-maximal inhibitory concentrations (IC<sub>50</sub> values) of Paclitaxel in a panel of 29 human primary lung-tumour-derived cell lines spanned a wide range of concentrations, from 1 nM to more than 1 mM (M.P., L.G. and J.D.M., unpublished observations). From this panel, we selected the NSCLC line NCI-H1155 for a genome-wide paclitaxel synthetic-lethal screen, given the IC<sub>50</sub> (about 50 nM) for this line, which is tenfold that observed for many other lines with similar proliferation rates. A high-efficiency, high-throughput short interfering RNA (siRNA) reverse transfection protocol was designed on the basis of our observations that transient trypsin-mediated suspension of adherent cultures markedly enhances the cellular uptake of liposome/nucleic acid particles<sup>2,3</sup> (Supplementary Fig. 1a).

We employed a library of 84,508 siRNAs corresponding to four unique siRNA duplexes, targeting each of 21,127 unique human genes

arrayed in a one-gene-one-well format on 96-well microtitre plates (Supplementary Table 1). Transfections were performed in sextuplicate for triplicate analysis in the presence and the absence of paclitaxel (Supplementary Fig. 1b). A 48-h exposure to 10 nM paclitaxel was used as an otherwise innocuous dose that was in range of a significant response at a tenfold higher drug concentration (Supplementary Fig. 1c). Cell viability was measured using ATP concentration, and raw values were normalized to internal reference control samples on each plate to permit plate-to-plate comparisons<sup>4</sup> (Supplementary Table 1 and Supplementary Fig. 1f). Each siRNA pool was assigned a viability ratio calculated as mean viability in paclitaxel divided by mean viability in the absence of drug (mean<sub>paclitaxel</sub>/mean<sub>carrier</sub>) (Supplementary Fig. 1d).

An objective protocol for the selection of significant 'hits' was derived to combine reproducibility of testing with magnitude of response (Supplementary Fig. 1e, and Methods described therein). First, we set a 5% false discovery rate (FDR) by using two-sample *t*-tests from the triplicate analysis together with *P*-value corrections for the multiplicity of testing<sup>5–8</sup> (Supplementary Table 2). Second, we selected all samples that both satisfied a 5% FDR and were present in the 2.5-centile rank of the viability ratios (Supplementary Table 3 and Supplementary Fig. 1e). A set of 87 candidate paclitaxel-sensitizer loci, defined as 'high-confidence hits', was identified that satisfied these criteria (Table 1). Retests of a subset of these candidates with independently synthesized siRNA pools reproduced a significant response to 10 nM paclitaxel (Fig. 1a).

A 5% FDR is a highly stringent cut-off that may produce many false negatives. Nonetheless, this cut off returned many candidates with overlapping functional relationships, including macromolecular complexes, receptor-ligand pairs, and products of related aberrant gene-expression programmes (Table 1, Fig. 1b–e, and Supplementary Table 4). Most striking was the presence of a large group of core components of the proteasome (Fig. 1b), consistent with numerous empirical observations of enhanced sensitivity to paclitaxel in cancer cells after proteasome inhibition. Multiple targets encoding proteins involved in the dynamics and function of microtubules were also isolated<sup>9</sup> (Table 1). Relaxing the FDR to 10% returned most of the known main components of the  $\gamma$ -tubulin ring complex ( $\gamma$ -TuRC), a central element of the microtubule organizing centres that nucleate the formation of the mitotic spindle<sup>10</sup> (Fig. 1c, and Supplementary Table 4). Isolation of these components is evocative of a successful primary screen, because the mitotic spindle apparatus is exquisitely sensitive to the inhibition of microtubule dynamics by paclitaxel and is probably the biologically relevant drug target in cancer cells<sup>11</sup>. The probabilities of this extent of enrichment of proteasome subunits and of  $\gamma$ -TuRC subunits by random chance are 1 in 10<sup>10</sup> ( $P \leq 0.0000000001$ )

<sup>1</sup>Department of Cell Biology, <sup>2</sup>Reata Pharmaceuticals, <sup>3</sup>Hamon Center for Therapeutic Oncology Research, <sup>4</sup>Simmons Cancer Center, <sup>5</sup>Department of Biochemistry, and <sup>6</sup>Center for Biostatistics and Clinical Science, University of Texas Southwestern Medical Center, Dallas, Texas 75390, USA.



**Table 1 | High-confidence hit list**

Symbol	Comments; motifs	Symbol	Comments; motifs
<b>Proteasome</b>		<b>Transcription</b>	
PSMA6	Proteasome subunit	RP9	ZnF_C2HC
PSMA7	Proteasome subunit	ZFPM1	ZnF_C2H2(x9)
PSMA8 (MGC26605)	Proteasome subunit	ZNF503	ZnF_C2H2
PSMB1	Proteasome subunit	ZNF585A	KRAB; ZnF_C2H2(x21)
PSMC3	Proteasome subunit	C11ORF30	ENT
PSMD1	Proteasome subunit	TRIM15	RING, BBOX, PRY, SPRY
PSMD3	Proteasome subunit		
<b>Microtubule-related</b>		<b>Translation</b>	
		RARSL	Arginyl-tRNA synthetase-like; Arg_S Core, tRNA-synt_1d_C
TUBGCP2	$\gamma$ -TURC subunit; Spc97_Spc98	LOC390876	Similar to 60S ribosomal protein L35; coiled-coil
TUBA8	$\alpha$ -Tubulin	LOC388568	Similar to ribosomal protein S15 isoform
DNHD1 (FLJ32752)	Dynein heavy-chain subunit	SYMPK	
DNAH10 (FLJ43808)	Dynein heavy-chain subunit	SYNCRIP	RRM
TBL1Y	Transducin ( $\beta$ )-like 1Y-linked; LisH, WD40	BCDIN3 (FLJ20257)	Bin3, PrmA
MPP7	MAGUK family; L27, PDZ_signalling, SH3, GMPK	LOC144233	Bin3
<b>Post-translational modification</b>		<b>Channel</b>	
FBXO18	FBOX, UvrD-helicase	ATP6V0D2	Lysosomal H <sup>+</sup> transporter; vATP-synt_AC39
RAI17	Similar to PIAS; zf-MIZ	SLC34A3	Solute carrier; Na_Pi_cotrans
RNF151	RING		
LOC389822 (DKFZp434E1818)	Transmembrane, RING	<b>Membrane protein</b>	
LOC401506 (new LOC648245)	RING	BEAN	Transmembrane, basic domain
HS6ST2	Heparan sulphotransferase	LRRTM1	LLRNT, LRR (x9), transmembrane
GAL3ST4	Galactose sulphotransferase	MGC31967	Transmembrane, C-C
MGC4655	Galactosyl_T	TMC05 (MGC35118)	Transmembrane, C-C
<b>Cell adhesion/ECM receptor</b>		<b>Other</b>	
PAPLN	Proteoglycan-like sulphated glycoprotein; TSP1.KU, IGcam	PDDC1 (FLJ34283)	GATase1_Hsp31_like
KIAA1920	Similar to chondroitin sulphate proteoglycan 4	C14ORF148	Predicted NADP oxidoreductase; P5CR
LRFN5	LRR, COG4886, IGcam, transmembrane	CWF19L2	Similar to CWF19; CwfJ_C_1, CwfJ_C_2
MGC33424	IG_FLMN, CAP10, KDEL	PRICKLE1	Planar cell polarity, nuclear receptor for REST; PET, LIM (x3)
C1QTNF3	C1q	CA10	Carbonic anhydrase; alpha_CARP_X_XI_like
ITIH5	VIT, vWA_interalpha_trypsin_inhibitor	FAM14B	Similar to ISG12, aIFN-inducible; Ifi-6-16
IGSF21 (MGC15730)	IGcam	TIP39	PTHR2 ligand
		HSN2	Hereditary sensory neuropathy locus
<b>Gametogenesis-associated/cancer testis antigens</b>		<b>Unknown</b>	
ACRBP	sp32, Kazal	NOD9	NACHT, LRR
FMR1NB	Transmembrane (x2), basic domain	F25965	
STARD6	START	LOC348262	
FSIP1	CC (x2)	C8orf33 (FLJ20989)	
<b>Receptor</b>		ANKRD41 (FLJ39369)	Ankyrin domains (ANK)
NTNG2	LamNT, EGF_Lam	CCDC38 (FLJ40089)	Coiled-coil
GPR144	PTX, GPS, 7transmembrane_2	C2orf33 (GL004)	DUF800
PDCL	Similar to phosducin	NLF1 (LOC145741)	NF- $\kappa$ B target gene
<b>Ras family</b>		BU077088 (LOC284409)	Transmembrane
FGD4	FYVE, RhoGEF and PH-domain-containing 4	BX103302 (LOC284931)	
FLJ32810	Rho_GAP, SH3	LOC340109	
SIPA1L2	Rap_GAP, PDZ_signalling	C21orf111 (LOC388830)	
RAB9A	RAB	LOC400236	
SYT13	Rab effector; C2	LOC400861	
		LOC55924	
		LOC56181	DUF729
		MGC10701	
		MGC15634	
		LOC56390 (LOC388497)	
		LOC257396	

and 1 in  $3 \times 10^9$  ( $\gamma$ -TuRC,  $P \leq 0.000000003$ ), respectively, as calculated by hypergeometric distribution analysis.

A surprising observation was the enrichment of genes, the expression of which is normally restricted to the testis. Four of these are known to encode tumour antigens that are markedly upregulated in many tumour types including NSCLC, breast cancer and melanoma (Fig. 1e;  $P \leq 0.003$  (hypergeometric distribution)). The restricted expression pattern and immunogenicity of cancer/testis antigens (CT antigens) has driven forward efforts for their use in cancer vaccines even in the absence of functional information<sup>12</sup>. Their identification in this screen suggests the obligatory participation of some CT antigens in aberrant cancer-cell regulatory programmes.

To probe the extent of chemosensitization that can be conferred by target gene depletion, a panel representing six functionally diverse groups from the 'high-confidence' hit list was selected. This panel included the following: CT-antigen ACRBP; the proteasome subunit PSMA6; the  $\gamma$ -TuRC protein TUBGCP2; a heparin sulphate transferase, HS6ST2, with significantly enriched expression in lung tumour tissue compared with normal lung (L.G. and J.D.M., unpublished observations); a vacuolar ATPase subunit, ATP6V0D2, expressed from a locus amplified in several lung cancer lines; and FGD4, a CDC42 activator. As controls for 'off-target' siRNA phenomena, we verified that each siRNA pool resulted in target gene knockdown, that at least two single siRNAs would recapitulate the phenotype

when tried separately, and that distinct pools of four more independent siRNAs against each gene also resulted in target knockdown and paclitaxel sensitization (Supplementary Fig. 2a–d).

We next examined the consequence of target depletion on responses to a broad range of concentrations of paclitaxel, vinorelbine and gemcitabine. Paclitaxel and vinorelbine impair mitotic spindle assembly through independent mechanisms that suppress microtubule dynamics<sup>11</sup>. In contrast, gemcitabine induces replication-stress-dependent apoptosis through DNA chain termination<sup>13</sup>. Several targets displayed significant collaboration with paclitaxel concentrations 1,000-fold below that used for the primary screen (Fig. 2a). Exposure to paclitaxel for a further 24–48 h magnified these differences: some groups responded to paclitaxel concentrations 10,000-fold lower than otherwise required (Fig. 2d). Cell survival curves and colony assays suggest that the decrease in cell number is a consequence of cell death rather than a transient delay in proliferation (Supplementary Fig. 3a, b). Some targets also significantly enhanced sensitivity to vinorelbine but, for the most part, only at concentrations at which vinorelbine alone detectably impaired cell viability (Fig. 2b). In contrast, target depletion had no remarkable

consequence on the maximally effective concentration of gemcitabine in H1155 cells, although the non-responding cell population was decreased or eliminated in all cases (Fig. 2c).

The apparent synergy that we observed between target depletion and paclitaxel, in comparison with other chemotherapeutic agents, suggests that genome-wide chemosensitizer screens return molecular components closely related to the mode of action of a particular drug. To test this directly, we examined the consequence of target depletion on the morphology of the mitotic spindle<sup>14</sup>. Depletion of FGD4 resulted in a significant accumulation of otherwise normal-appearing mitotic figures in the absence of paclitaxel, indicating that this protein may be required for support of mitotic progression (Supplementary Fig. 4). Depletion of ACRBP and TUBGCP2, although not detectably affecting mitosis in the absence of drug, resulted in a marked accumulation of multipolar spindles in the presence of 10 nM paclitaxel (Fig. 3a, and Supplementary Fig. 5b). Multipolar spindle accumulation is typical after exposure to higher doses of paclitaxel in H1155 cells as well as in other cancer cell types<sup>9,11</sup> (data not shown). Simultaneous depletion of MAD2, an obligate component of the spindle assembly checkpoint<sup>14</sup>, reversed the accumulation of mitotic figures with the concomitant appearance

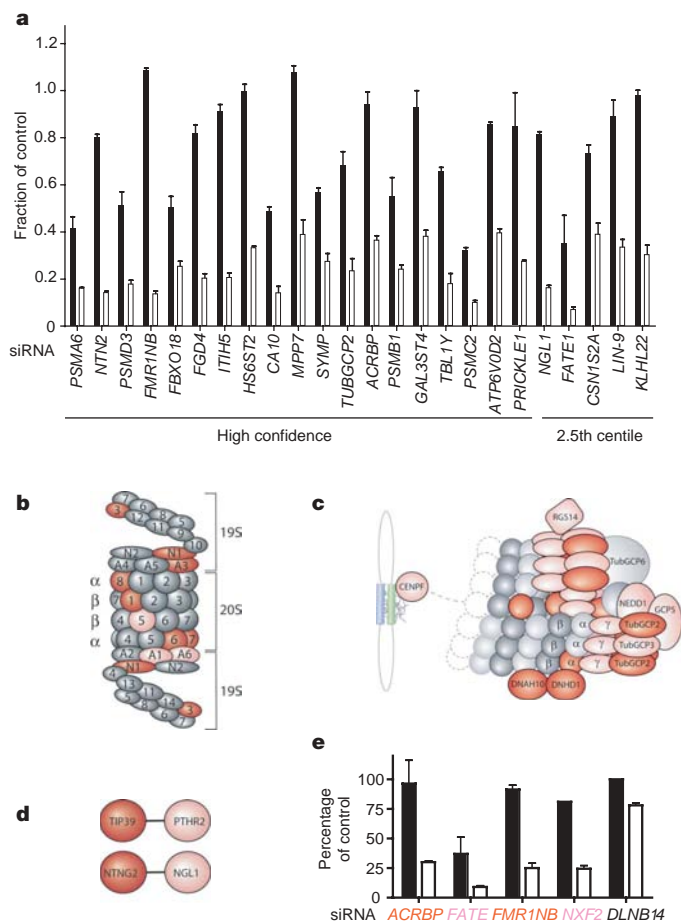


**Figure 1 | Functional relationships among candidate paclitaxel-sensitizing siRNA targets.** **a**, Retests of a panel of independently synthesized siRNA pools targeting candidate genes that modulate paclitaxel sensitivity. Results are cell viability normalized to control siRNA-transfected samples and are shown as means and s.e.m. for  $n = 3$ . Black bars, no paclitaxel; white bars, 10 nM paclitaxel. **b**, Proteasome. Red shading indicates satisfaction of 5% FDR, pink shading indicates satisfaction of 10% FDR. **c**,  $\gamma$ -TuRC and related components of the mitotic spindle apparatus. Shading is as in **b**. **d**, Ligand-receptor pairs. Shading is as in **b**. **e**, CT antigens. Results are viability normalized as a percentage of control siRNA transfected samples (DLNB14) and are shown as means and s.e.m. Black bars, 0 nM paclitaxel; white bars, 10 nM paclitaxel. siRNA gene shading is as in **b**. Values are representative of a minimum of three independent experiments.

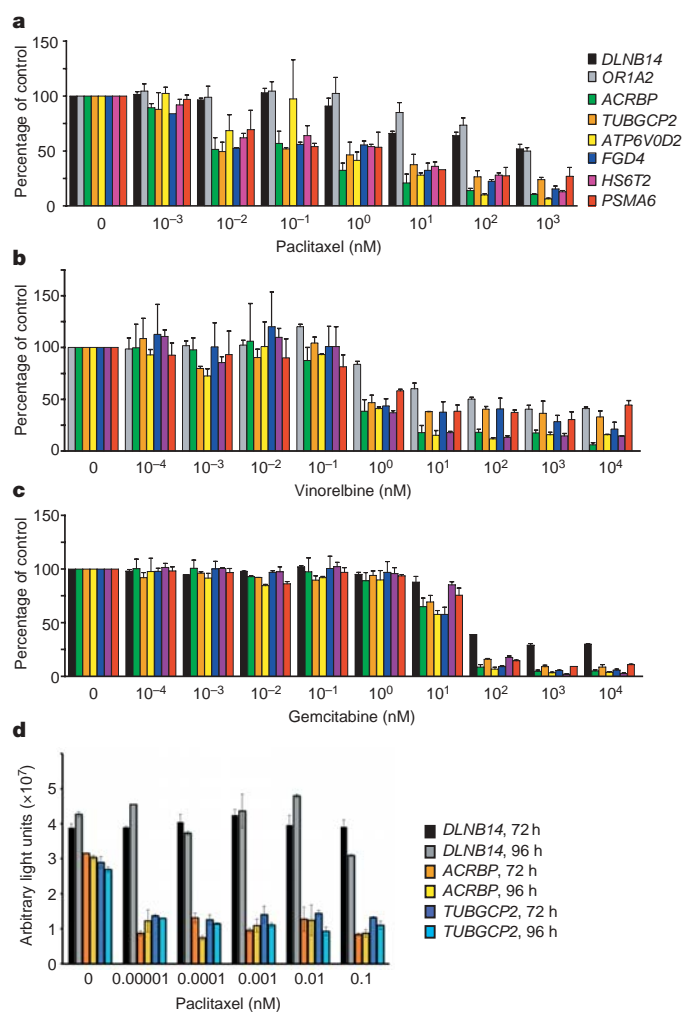


**Figure 2 | Drug sensitivity profiles.** **a–c**, H1155 transfected with siRNAs targeting the indicated genes (DLNB1 and OR1A2 are control siRNAs) were exposed to paclitaxel (a), vinorelbine (b) or gemcitabine (c) 48 h after transfection at the indicated doses for 48 h. Results are viability normalized to siRNA-transfected samples in the absence of drug and are shown as means and s.e.m. Values are representative of three independent experiments. **d**, H1155 transfected with siRNAs targeting the indicated genes were treated with paclitaxel 48 h after transfection for the indicated times. Bars are cell viability obtained with Cell Titer Glo and are shown as means and s.e.m.

of numerous micronucleated cells, indicating mitotic slippage through a defective spindle assembly checkpoint (Fig. 3a). Depletion of PSMA6, HS6ST2 and ATP6V0D2 did not affect mitotic spindle assembly (data not shown).

Given the significant genetic heterogeneity between cancer cell lines we next examined the effect of target depletion on a panel of lung lines, with diverse paclitaxel  $IC_{50}$  values, that included the NSCLC line HCC4017 and normal, non-malignant bronchial epithelial line HBE30 (ref. 15), isolated from the same individual. Out of 12 targets tested with the patient-matched tumour and normal lines, the depletion of 4 targets selectively sensitized the tumour-derived line to low-dose paclitaxel (Supplementary Fig. 5a). Two of the four sensitizers were in the CT-antigen family. Three out of four CT antigens tested also sensitized at least one additional NSCLC line to low-dose paclitaxel with no measurable consequences on the viability of HBE30 cells. Not surprisingly, proteasome subunit depletion was

broadly effective in tumour cells in comparison with normal cells (Supplementary Fig. 5a).

We also examined the effect of ACRBP or TubGCP2 depletion on mitotic progression in these lines. Although neither ACRBP nor TUBGCP2 depletion affected cell viability as assessed by ATP concentration in H1299 and H2126 NSCLC cells, depletion of these targets did enhance paclitaxel-induced mitotic arrest (Supplementary Fig. 5b). The lack of change in viability may reflect differences in the coupling of spindle assembly checkpoint machinery to apoptosis in different cancer cell lines<sup>16</sup>. Consistent with this was our observation that depleting ACRBP or TUBGCP2 sensitized H1155 cells to paclitaxel-induced caspase activation (Supplementary Fig. 5d), whereas in H2126 cells, depletion of ACRBP collaborated with paclitaxel to inhibit proliferation (Supplementary Fig. 6a). In addition, the depletion of either ACRBP or TUBGCP2 in lung-tumour-derived cell lines lacking a robust spindle assembly checkpoint (HCC366, HCC15 or HCC4017) was sufficient to induce the accumulation of non-proliferating micronucleated cells, which are normally observed after exposure to paclitaxel (Fig. 3c, and Supplementary Fig. 6b, c). These observations highlight the emerging concept that products of anomalous gene-expression programmes can become engaged to buttress the fundamental biological systems required for the proliferative fitness of cancer cells. In a specific sense, aberrant expression of proteins such as ACRBP may contribute to mitotic progression in cancer cells by enhancing the robustness of an otherwise weakened mitotic spindle apparatus.

An expected outcome of genomic chemosensitizer screens is the identification of gene products that are targets of currently available compounds, indicating novel combinatorial therapeutic regimens. Our isolation of the proteasome exemplifies this relationship because collaboration between bortezomib, a proteasome inhibitor, and paclitaxel has been demonstrated clinically<sup>17</sup>. Isolation of ATP6V0D2, a subunit of the vacuolar ATPase (V-ATPase)<sup>18</sup> (Table 1 and Fig. 1a), predicts that lysosomal ATPase-inhibitors may be effective cytotoxic agents in combination with paclitaxel. Salicylhalamide A was originally identified as an anti-tumour agent and was subsequently found to target V-ATPase activity directly<sup>19,20</sup>. Exposure of H1155 cells to increasing doses of a synthetic salicylhalamide derivative<sup>21</sup>, RTA 203, together with low-dose paclitaxel revealed a significant collaborative impact on viability at doses well below that required for the activity of a single agent (Fig. 3d, e). This observation highlights the strong predictive power of genome-wide synthetic-lethal screens for identification of productive drug–drug interactions. We have used a high-throughput functional-genomics screening platform, together with an objective ‘hit’ selection criterion derived from probabilistic judgments of error rates, to produce an unbiased and high-confidence collection of the molecular components modulating chemosensitivity in lung cancer cells. The results reveal major fulcrums of the autonomous response of cancer cells to abrogation of microtubule dynamics; the results also identify therapeutic targets for combinatorial chemotherapy and highlight a major contribution of cancer-associated anomalous gene expression patterns for support of mitotic progression in cancer cells.

## METHODS

All cells were reverse-transfected with siRNA pools complexed with DharmaFECT reagent (optimized for each cell type). Cells were treated 48 h after transfection and viability was assessed after an additional 48 h. For screening data analysis, each siRNA pool was assigned a viability ratio. Viability ratios were ranked by reproducibility between three replicates for each condition, using a two-sample *t*-test followed by a Benjamini–Hochberg correction. Immunofluorescence was performed with the use of standard fixation and permeabilization protocols. Cells were stained with monoclonal  $\beta$ -tubulin antibodies, polyclonal pericentrin antibodies, bromodeoxyuridine or antibodies against cleaved caspase-3 followed by secondary labelling with secondary fluorescein isothiocyanate-conjugated anti-mouse antibodies or tetramethylrhodamine  $\beta$ -isothiocyanate-conjugated anti-rabbit antibodies. Cells were observed under a Zeiss Axioplan 2E microscope equipped with a Hamamatsu monochrome

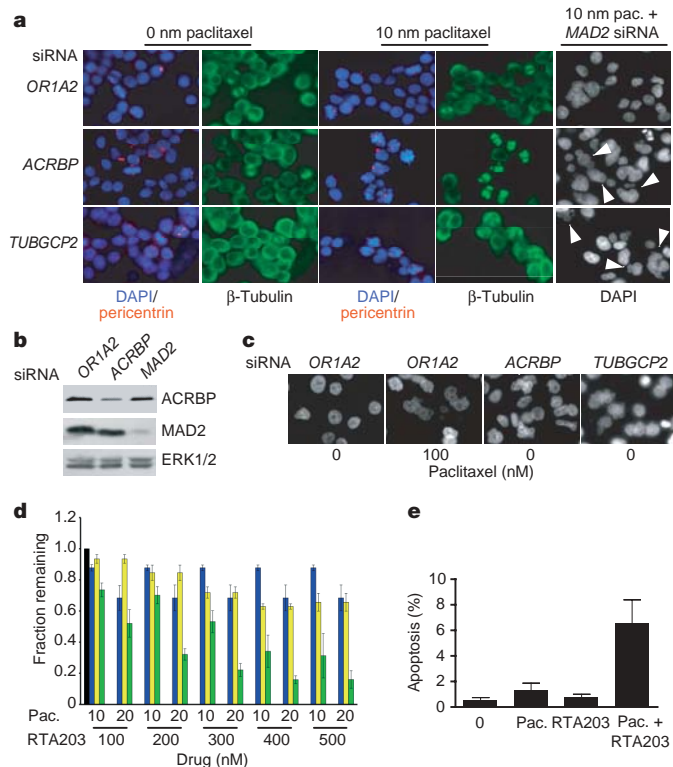


**Figure 3 | Convergence of paclitaxel and sensitizer gene function on mitotic spindle integrity.** **a**, At 48 h after transfection with the indicated siRNAs, H1155 cells were exposed to the indicated paclitaxel concentrations for 24 h. Microtubules, genomic DNA and centrosomes were revealed by immunostaining with  $\beta$ -tubulin, 4,6-diamidino-2-phenylindole (DAPI) and  $\alpha$ -pericentrin, respectively. Arrowheads indicate the formation of micronuclei as a consequence of bypass of MAD2-dependent mitotic spindle checkpoint arrest. Pictures are representative of a minimum of five independent experiments. Pac., paclitaxel. **b**, siRNA-dependent depletion of ACRBP and MAD2 was verified by immunoblots of whole-cell lysates from **a**. **c**, The interphase nuclear morphology of HCC366 cells transfected with the indicated siRNAs was examined with DAPI. Arrowheads indicate cells containing multiple micronuclei. Pictures are representative of a minimum of three independent experiments. **d**, Collaborative impact of paclitaxel and RTA-203 on H1155 cell viability. Results are viability normalized to untreated control samples (black bar) and are shown as means and s.e.m. Yellow bars, RTA-203 alone; blue bars, paclitaxel alone; green bars, RTA-203 plus paclitaxel at the indicated doses. Values are representative of three independent experiments. **e**, Percentage apoptosis as indicated by cleaved caspase-3 immunostaining of H1155 cells after a 24-h exposure to 10 nM paclitaxel or 200 nM RTA-203, or a combination of both. Error bars show s.e.m. for four independent experiments.

digital black-and-white camera and Open Lab Software. Quantitative polymerase chain reaction was performed on RNA extracted from all cells with the Roche LightCycler System or the 7900HT Fast Real-Time PCR System with primers flanking at least two siRNA target sequences and lying on separate exons. Growth inhibition assays were performed with a Sulphorhodamine B protocol on cells treated for 48 hours with the indicated drugs<sup>22</sup>. For colony formation assays, transfected and treated cells were replated and stained with Geimsa 5 days later. Immunoblots were performed on whole-cell lysates from H1155 cells with the use of standard protocols.

A detailed description of the screening strategy and statistical analysis is given in Supplementary Fig. 1 and Supplementary Methods. Optimized transfection protocols and growth conditions for the multiple cell lines used in this study are described in Supplementary Table 6. siRNA sequences and reverse transcriptase-mediated polymerase chain reaction primers are described in Supplementary Tables 5 and 7. Methods for standard viability assays and quantification of mitotic progression are also included in Supplementary Methods.

**Received 26 October 2006; accepted 20 February 2007.**

- Green, D. R. & Evan, G. I. A matter of life and death. *Cancer Cell* **1**, 19–30 (2002).
- Chien, Y. & White, M. A. RAL GTPases are linchpin modulators of human tumour-cell proliferation and survival. *EMBO Rep.* **4**, 800–806 (2003).
- Matheny, S. A. *et al.* Ras regulates assembly of mitogenic signalling complexes through the effector protein IMP. *Nature* **427**, 256–260 (2004).
- Malo, N., Hanley, J. A., Cerquozzi, S., Pelletier, J. & Nadon, R. Statistical practice in high-throughput screening data analysis. *Nature Biotechnol.* **24**, 167–175 (2006).
- Benjamini, Y. H. Y. Controlling the false discovery rate: a practical and powerful approach to multiple testing. *J. R. Statist. Soc. B* **57**, 289–300 (1995).
- Allison, D. B., Cui, X., Page, G. P. & Sabripour, M. Microarray data analysis: from disarray to consolidation and consensus. *Nature Rev. Genet.* **7**, 55–65 (2006).
- Wit, E. & McClure, J. Statistical adjustment of signal censoring in gene expression experiments. *Bioinformatics* **19**, 1055–1060 (2003).
- Benjamini, Y. & Hochberg, Y. Controlling the false discovery rate: a practical and powerful approach to multiple testing. *J. R. Statist. Soc. B* **57**, 289–300 (1995).
- Jordan, M. A. & Wilson, L. The use and action of drugs in analyzing mitosis. *Methods Cell Biol.* **61**, 267–295 (1999).
- Moritz, M. & Agard, D. A. Gamma-tubulin complexes and microtubule nucleation. *Curr. Opin. Struct. Biol.* **11**, 174–181 (2001).
- Jordan, M. A. & Wilson, L. Microtubules as a target for anticancer drugs. *Nature Rev. Cancer* **4**, 253–265 (2004).
- Scanlan, M. J., Simpson, A. J. & Old, L. J. The cancer/testis genes: review, standardization, and commentary. *Cancer Immun.* **4**, 1–15 (2004).
- Toschi, L., Finocchiaro, G., Bartolini, S., Gioia, V. & Cappuzzo, F. Role of gemcitabine in cancer therapy. *Future Oncol.* **1**, 7–17 (2005).
- Weaver, B. A. & Cleveland, D. W. Decoding the links between mitosis, cancer, and chemotherapy: The mitotic checkpoint, adaptation, and cell death. *Cancer Cell* **8**, 7–12 (2005).
- Ramirez, R. D. *et al.* immortalization of human bronchial epithelial cells in the absence of viral oncoproteins. *Cancer Res.* **64**, 9027–9034 (2004).
- Rieder, C. L. & Maiato, H. Stuck in division or passing through: what happens when cells cannot satisfy the spindle assembly checkpoint. *Dev. Cell* **7**, 637–651 (2004).
- Davies, A. M. *et al.* Bortezomib-based combinations in the treatment of non-small-cell lung cancer. *Clin. Lung Cancer* **7** (Suppl 2), S59–S63 (2005).
- Kawasaki-Nishi, S., Nishi, T. & Forgac, M. Proton translocation driven by ATP hydrolysis in V-ATPases. *FEBS Lett.* **545**, 76–85 (2003).
- Boyd, M. R. *et al.* Discovery of a novel antitumor benzolactone enamide class that selectively inhibits mammalian vacuolar-type (H<sup>+</sup>)-ATPases. *J. Pharmacol. Exp. Ther.* **297**, 114–120 (2001).
- Xie, X. S. *et al.* Salicylihalamide A inhibits the VO sector of the V-ATPase through a mechanism distinct from bafilomycin A1. *J. Biol. Chem.* **279**, 19755–19763 (2004).
- Wu, Y., Liao, X., Wang, R., Xie, X. S. & De Brabander, J. K. Total synthesis and initial structure–function analysis of the potent V-ATPase inhibitors salicylihalamide A and related compounds. *J. Am. Chem. Soc.* **124**, 3245–3253 (2002).
- Skehan, P. *et al.* New colorimetric cytotoxicity assay for anticancer-drug screening. *J. Natl Cancer Inst.* **82**, 1107–1112 (1990).

**Supplementary Information** is linked to the online version of the paper at [www.nature.com/nature](http://www.nature.com/nature).

**Acknowledgements** This work was supported by grants from the National Cancer Institute, the Robert E. Welch Foundation, the Susan G. Komen Foundation, the Department of Defense Congressionally Directed Medical Research Program and the National Cancer Institute Lung Cancer Specialized Program of Research Excellence.

**Author Information** Reprints and permissions information is available at [www.nature.com/reprints](http://www.nature.com/reprints). The authors declare no competing financial interests. Correspondence and requests for materials should be addressed to M.A.W. ([michael.white@utsouthwestern.edu](mailto:michael.white@utsouthwestern.edu)).